

# Purification and Characterization of a New RGD/KGD-Containing Dimeric Disintegrin, Piscivostatin, from the Venom of *Agkistrodon piscivorus piscivorus*: The Unique Effect of Piscivostatin on Platelet Aggregation<sup>1</sup>

Daiju Okuda and Takashi Morita<sup>2</sup>

Department of Biochemistry, Meiji Pharmaceutical University, 2-522-1 Noshio, Kiyose, Tokyo 204-8588

Received May 22, 2001; accepted June 21, 2001

**Piscivostatin, a novel dimeric disintegrin containing Arg-Gly-Asp (RGD) and Lys-Gly-Asp (KGD) sequences, was isolated from the venom of *Agkistrodon piscivorus piscivorus*. The molecule consisted of two chains designated as the  $\alpha$  and  $\beta$  chains, comprising 65 and 68 amino acid residues, respectively. Piscivostatin had two binding motifs recognized by platelet glycoprotein IIb/IIIa (GPIIb/IIIa), and the biological activity of dimeric disintegrin piscivostatin toward platelet aggregation differed from those of other monomeric disintegrins such as trimestatin and echistatin. We measured platelet aggregation by the laser light scattering method during the process of ADP-induced platelet aggregation. Both dimeric and monomeric disintegrins inhibited the formation of small (9 to 25  $\mu$ m in diameter), medium-sized and large aggregates (25 to 70  $\mu$ m in diameter) in a dose-dependent manner. The platelet aggregates disaggregated after reaching a maximal number on either treatment with ADP alone or monomeric disintegrin/ADP. However, the small aggregates did not disaggregate on treatment with piscivostatin/ADP even when applied over time. When washed platelets were incubated with an anti-GPIIb/IIIa monoclonal antibody, PT25-2, which induces conformational changes of GPIIb/IIIa to a form accessible to fibrinogen and other adhesion proteins without platelet activation, piscivostatin induced a platelet shape change alone with no aggregate formation. The present study indicated that piscivostatin has two unique contradictory activities; acting as a double inhibitor of platelet aggregation and platelet aggregate dissociation.**

**Key words:** ADP-induced platelet aggregation, disintegrin, laser-light scattering, platelet shape change, snake venom.

Platelets play an important role in hemostasis as an essential component of the initial hemostatic plug at the sites of injury (1). After platelets have been activated by various physiological agonists, they bind to fibrinogen and then form aggregates *via* platelet glycoprotein IIb/IIIa (GPIIb/IIIa), which is a calcium-dependent heterodimeric complex on the platelet membrane. The interaction of fibrinogen and the receptor is inhibited by short synthetic peptides bearing the RGD sequence, which is the smallest motif for binding to GPIIb/IIIa and other integrins (2–4).

Disintegrins of snake venoms are small cysteine-rich peptides containing Arg-Gly-Asp (RGD) or Lys-Gly-Asp (KGD), a platelet GPIIb/IIIa binding motif, and act as potent platelet aggregation inhibitors. Many disintegrins from the venoms of various snakes have been isolated and characterized (5–7). These molecules exhibit not only anti-platelet aggregation activity but also show binding activity toward some integrins such as integrin  $\alpha$ v $\beta$ 1, a vitronectin receptor, and integrin  $\alpha$ 5 $\beta$ 1, a fibronectin receptor. These disintegrins are also used as research tools in studies on cell–cell interactions and cancer metastasis (8, 9).

Venom disintegrins are classified into three types according to their molecular size: echistatin (10) and ristocetin (11) are small type disintegrins with molecular weights of about 5 to 6 kDa (approximately 50 amino acids); trigramin (12) and kistrin (13) are medium-sized disintegrins with molecular weights of about 7 to 8 kDa (approximately 70 amino acids); and bitistatin (14) is the largest monomeric disintegrin with a molecular weight of about 9 kDa (approximately 80 amino acids). These molecules show a high degree of amino acid sequence identity, and the disulfide bridge patterns of echistatin (15, 16), flavoridin (17), kistrin (18), and bitistatin (19), which were identified by means of NMR and enzymatic digestion, are highly similar. With a

<sup>1</sup> This work was supported in part by a grant from the Japan Health Sciences Foundation, and by Scientific Research Grants-in-Aid from the Ministry of Education, Science and Culture of Japan.

<sup>2</sup> To whom correspondence should be addressed. Phone: +81-424-95-8479, Fax: +81-424-95-8479, E-mail: tmorita@my-pharm.ac.jp

Abbreviations: PVS, piscivostatin; RGD, arginine-glycine-aspartate; KGD, lysine-glycine-aspartate; GPIIb/IIIa, glycoprotein IIb/IIIa; PAGE, polyacrylamide gel electrophoresis; PRP, platelet-rich plasma; PPP, platelet-poor plasma; PGI<sub>2</sub>, prostaglandin I<sub>2</sub>; LS, laser-light scattering; LSI, light scattering intensity; MALDI-TOF MS, matrix-assisted laser desorption/ionization time of flight mass spectrometry; CTS, contortrostatin; US-2, ussuristatin 2.

few exceptions, disintegrins with the RGD or KGD sequence have monomeric structures. Contortrostatin of the venom of *Aghkistrodon contortrix contortrix* has been suggested to be a homodimeric disintegrin (20), and its cDNA sequence has been reported (21). Ussuristatin-2 of the venom of *Aghkistrodon ussuriensis* has also been reported to be a homodimeric disintegrin containing the KGD sequence (22). EMF10 was most recently isolated from the venom of *Eristocophis macmahoni* (23). It has the RGD sequence in its A chain and the MGD sequence instead of the RGD sequence in its B chain (23).

In the present study, we isolated and characterized a novel RGD- and KGD-containing dimeric disintegrin designated as piscivostatin (PVS) from the venom of *Aghkistrodon piscivorus piscivorus*. This is the first study demonstrating the effects of both monomeric and dimeric disintegrins on the reversible phase of platelet aggregation, as judged with a laser-light scattering method. The new dimeric disintegrin, PVS, is the first RGD/KGD-containing dimeric disintegrin, and has a novel effect, preventing the dissociation of platelet aggregates, on ADP-induced platelet aggregation.

#### MATERIALS AND METHODS

**Materials**—The suppliers of the materials used in this study were as follows. The lyophilized venom of *A. piscivorus piscivorus* was purchased from Kentucky Reptile Zoo (KY, USA); Superdex 75 pg and SP-Sepharose High Performance FPLC columns from Pharmacia LKB Biotechnology Inc.; the COSMOSIL 5C18 AR-300 HPLC column from Nacalai Tesque (Kyoto); endoprotease Lys-C from Seikagaku Corporation (Tokyo); Endoprotease Asp-N and endoprotease Glu-C from Boehringer Mannheim (Marburg, Germany); ADP and echistatin from Sigma (MO, USA); and prostaglandin I<sub>2</sub> (PGL<sub>2</sub>) from Cayman Chemical Company (MI, USA). The other chemicals used in this study were purchased from Sigma and Wako Pure Chemical Corporation (Osaka), and Kanto Chemical Corporation (Tokyo). PT25-2, an anti-human GPIIb/IIIa monoclonal antibody (24), was a kind gift from Dr. Makoto Handa (Keio University, Tokyo). GPIIb/IIIa was purified from out-of-date human platelets, a kind gift from the Japanese Red Cross, by the method of Phillips *et al.* (25). Trimestatin is a monomeric disintegrin that was identified and purified from the venom of *Trimeresurus flavoviridis* in our laboratory. The amino acid sequence of trimestatin differs in only one amino acid residue in its C-terminal region from that of triflavin (26), which was purified from the same venom. Triflavin has a Gly as residue 69, while trimestatin has Asp at the corresponding position. Other sequences of these disintegrins are identical. The amino acid sequence of trimestatin is shown in Fig. 8.

**Purification of Piscivostatin**—One gram of lyophilized venom was dissolved in 50 mM Tris-HCl buffer (pH 8.0), insoluble materials being removed by centrifugation. The supernatant was applied to a column of Superdex 75 pg (1.6 × 60 cm) pre-equilibrated with the same buffer and eluted at a flow rate of 1 ml/min. Fractions were assayed for inhibitory activity toward ADP-induced aggregation of human platelets. The active fractions were pooled and then loaded onto a column of SP-Sepharose High Performance (1.6 × 10 cm) pre-equilibrated with 20 mM imidazole-HCl buffer (pH 6.8). The column was washed with the same

buffer and developed with a linear gradient of NaCl (0–0.4 M) in the same buffer over 80 min at a flow rate of 2 ml/min. The active fractions were pooled and loaded onto a preparative COSMOSIL 5C18 reverse-phase HPLC column (0.45 × 25 cm) equilibrated with 0.1% (v/v) trifluoroacetic acid in water. The column was developed at room temperature with a linear acetonitrile gradient in 0.1% aqueous trifluoroacetic acid at a flow rate of 1 ml/min.

**SDS-Polyacrylamide Gel Electrophoresis (SDS-PAGE)**—The apparent  $M_r$  of PVS was estimated using a Tris-tricine 16% gel with molecular weight markers (Pharmacia Biotech) according to the protocol of Schägger and von Jagow (27) under reducing and nonreducing conditions.

**Amino Acid Sequence Analysis**—Piscivostatin was reduced for 1 h at room temperature with 20 mM dithiothreitol in the presence of 0.5 M Tris-HCl, 6 M guanidinium hydrochloride and 2 mM EDTA (pH 8.3) in a volume of 0.5 ml. 4-Vinylpyridine was then added and alkylation was allowed to proceed for 1 h at room temperature. The S-pyridylethylated  $\alpha$  chain and  $\beta$  chain(s) of PVS were separated from reagents by C18 reverse-phase HPLC, and then their complete amino acid sequences were determined by sequencing of the peptides obtained on digestion with endoprotease Asp-N, endoprotease Lys-C, and endoprotease Glu-C. All samples were analyzed with Applied Biosystems protein sequencers (models 473A and 477A).

**Assaying of Binding of Disintegrins to Platelet GPIIb/IIIa**—250 ng aliquots of soluble GPIIb/IIIa were immobilized on 96-well plates at 4°C overnight. Various concentrations of PVS and trimestatin were allowed to bind to the immobilized GPIIb/IIIa at 37°C for 1 h. The bound disintegrins were detected with specific polyclonal antibodies (1  $\mu$ g/ml) against each disintegrin. Peroxidase-conjugated goat anti-rabbit antibodies were used as the secondary antibodies. The reaction of the antibodies with the antigen was visualized by incubation with *o*-phenylenediamine and the absorbance at 492 nm was recorded. The  $K_d$  values of disintegrins were obtained from double-reciprocal plots.

**Platelet Aggregation Studies**—Total human blood was obtained from healthy volunteers with informed consent; all the volunteers denied taking any medication. The study protocols were approved by the Ethics Committee of our university. Blood was collected from volunteers, in a 0.1 volume of 3.8 w/v% sodium citrate, by venipuncture and then centrifuged at 150  $\times$ g for 20 min at room temperature to prepare platelet-rich plasma (PRP). Platelet-poor plasma (PPP) was separated from PRP by further centrifugation at 300  $\times$ g for 5 min. Washed platelets were prepared by further centrifugation of PRP, washed twice with 10% ACD (acid/citrate/dextrose) and 100 nM PGL<sub>2</sub>, and then resuspended in Hepes-tyrode buffer, which comprised 20 mM Hepes, pH 7.4, 138 mM NaCl, 3.3 mM NaH<sub>2</sub>PO<sub>4</sub>, 2.9 mM KCl, 1.0 mM MgCl<sub>2</sub>, and 1 mg/ml glucose. The platelet suspension was supplemented with 1 mM CaCl<sub>2</sub> at 20 min before the experiments. Disintegrin was added to the platelets and then the mixture was incubated at 37°C, followed by the addition of ADP (final concentration, 10  $\mu$ M) or fibrinogen (final concentration, 1 mg/ml), when using PT25-2 treated washed platelets, to initiate aggregation. Platelet aggregation was measured by determining the changes in light transmission with an optical aggregometer (Niko Bioscience Hema Tracer 601) and AG-10 (Kowa, Tokyo).

The principles of the light scattering (LS) method for

determining the total light scattering intensities (LSI) of small, medium-sized, and large aggregates were described previously (28). Particles with an intensity of 25 to 400 mV represented small aggregates (9–25  $\mu\text{m}$ ), ones with an intensity of 400 to 1,000 mV medium-sized aggregates (25–50  $\mu\text{m}$ ), and ones with an intensity of 1,000 to 2,048 mV large aggregates (50–70  $\mu\text{m}$ ). In the presence of ADP, small aggregates contained approximately 50–1,000 platelets, medium-sized aggregates approximately 1,000–9,000 platelets, and large aggregates 9,000–25,000 platelets.

## RESULTS

**Purification of Piscivostatin**—We assessed the presence of disintegrin(s) in the venom of *A. piscivorus piscivorus* by means of a platelet aggregation inhibitory assay with PRP in each column chromatography step, Superdex 75 pg, SP-Sepharose High Performance, and reversed-phase HPLC C18 columns being used. Two platelet aggregation inhibitors were finally isolated by reversed-phase HPLC (Fig. 1). We designated these proteins as piscivostatin 1 (PVS1) and piscivostatin 2 (PVS2), which were eluted in peak 1 with 25% and in peak 2 with 26% acetonitrile from the HPLC column (Fig. 1). The yields of PVS1 and PVS2 were 3.4 mg and 6.9 mg from 1 g of venom, respectively. The  $M_r$  on SDS-PAGE of PVS1 and PVS2 were 16 kDa under nonreducing conditions and 8 kDa under reducing conditions (inset in Fig. 1).

**Characterization of PVS**—The *S*-pyridylethylated PVS2 was separated into three peaks on C18 HPLC (Fig. 2A); the  $\alpha$ ,  $\beta$ , and  $\beta'$  chains were eluted at 19, 22, and 23% acetonitrile,

respectively. The  $M_r$  of the  $\alpha$  and  $\beta$  chains were determined to be 6.2 and 5.9 kDa by SDS-PAGE (Fig. 2B), and the  $M_r$  of the  $\beta'$  chain was identical to that of the  $\beta$  chain (data not shown). The chromatographic pattern of PVS1 was almost identical to that of PVS2, the exception being that the amount of the  $\beta'$  chain of PVS1 was much lower than that of PVS2 (data not shown). The amino acid sequences of PVS1 and PVS2 were determined by N-terminal Edman degradation of each *S*-pyridylethylated sample, and endoprotease Lys-C, endoprotease Asp-N and endoprotease Glu-C digested fragments. These fragments were purified by HPLC after digestion. The complete amino acid sequences of PVS1 and PVS2 are shown in Fig. 3. PVS1 was composed of an  $\alpha$  chain comprising 64 amino acids and a  $\beta$  chain comprising 64 amino acids (Fig. 3A), and the  $\alpha$ ,  $\beta$ , and  $\beta'$  chains of PVS2 comprised 65, 68, and 64 amino acids (Fig. 3B), respectively. The amino terminus of the  $\beta'$  chain of PVS2 started from four residues downstream of that of the  $\beta$  chain, the remainder of the amino acid sequence being completely identical to those of the  $\beta$  chains of both PVS1 and PVS2. The  $\beta'$  chain was most likely a protease-degraded form of the  $\beta$  chain. In PVS2, heterogeneity was detected at residue 56 (N/D) of the  $\beta$  chain and residue 52 (N/D) of the  $\beta'$  chain (Fig. 3B). The ratios of both residue 56N to 56D in the  $\beta$  chain and residue 52N to 52D in the  $\beta'$  chain were approximately 7:1, respectively. The  $\alpha$  chains of PVS1 and PVS2 had identical sequences except for the C-terminal residue, and the  $\beta$  chains of PVS1 and PVS2 were also identical except for the N-terminal residue. The sequence identity between the  $\alpha$  and  $\beta$  chains of PVS2 was 66% (Fig. 3C). The  $\alpha$  chain contained the Arg-Gly-Asp (RGD) sequence and the  $\beta$  chain contained Lys-Gly-Asp (KGD) as the GPIIb/IIIa binding sites. Both chains of PVS1 and PVS2 contained 10 cysteine residues, and the alignment of the Cys residues was identical. The amino acid sequence of PVS1 was also identical to that of PVS2 except

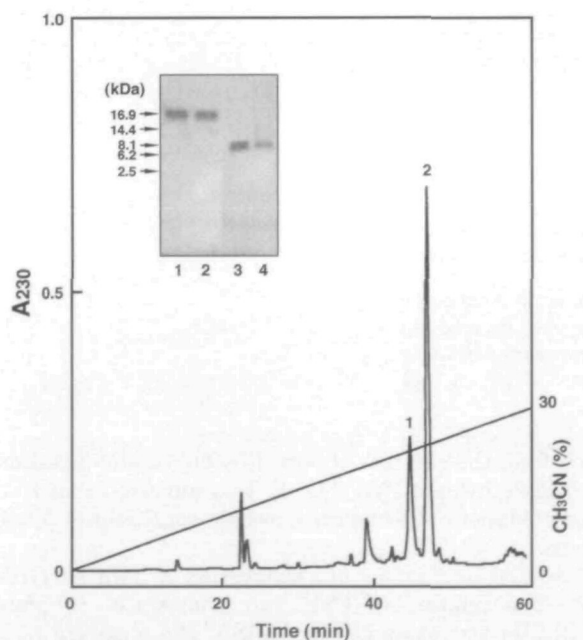


Fig. 1. Purification of piscivostatin. The active fractions obtained on SP-Sepharose HP chromatography were pooled and applied to a reverse phase C18 HPLC column as described under "MATERIALS AND METHODS." The numbers above the peaks indicate piscivostatins 1 and 2. The results of SDS-PAGE are shown in the inset: lanes 1 and 3, nonreduced and reduced piscivostatin 1, respectively; lanes 2 and 4, nonreduced and reduced piscivostatin 2, respectively. The arrows at the left indicate the  $M_r$  of molecular standards.

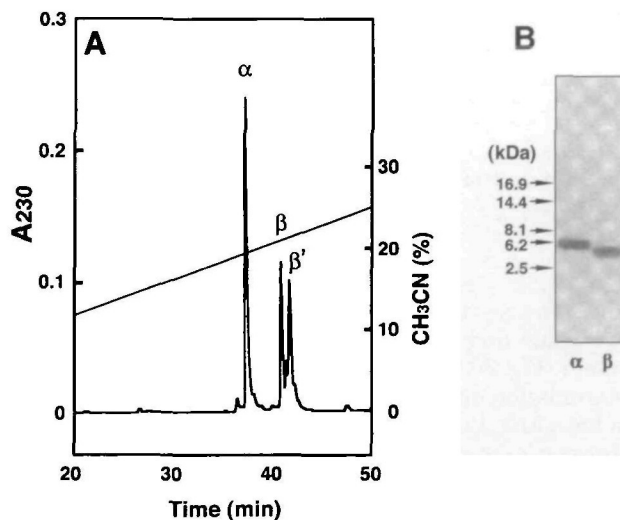
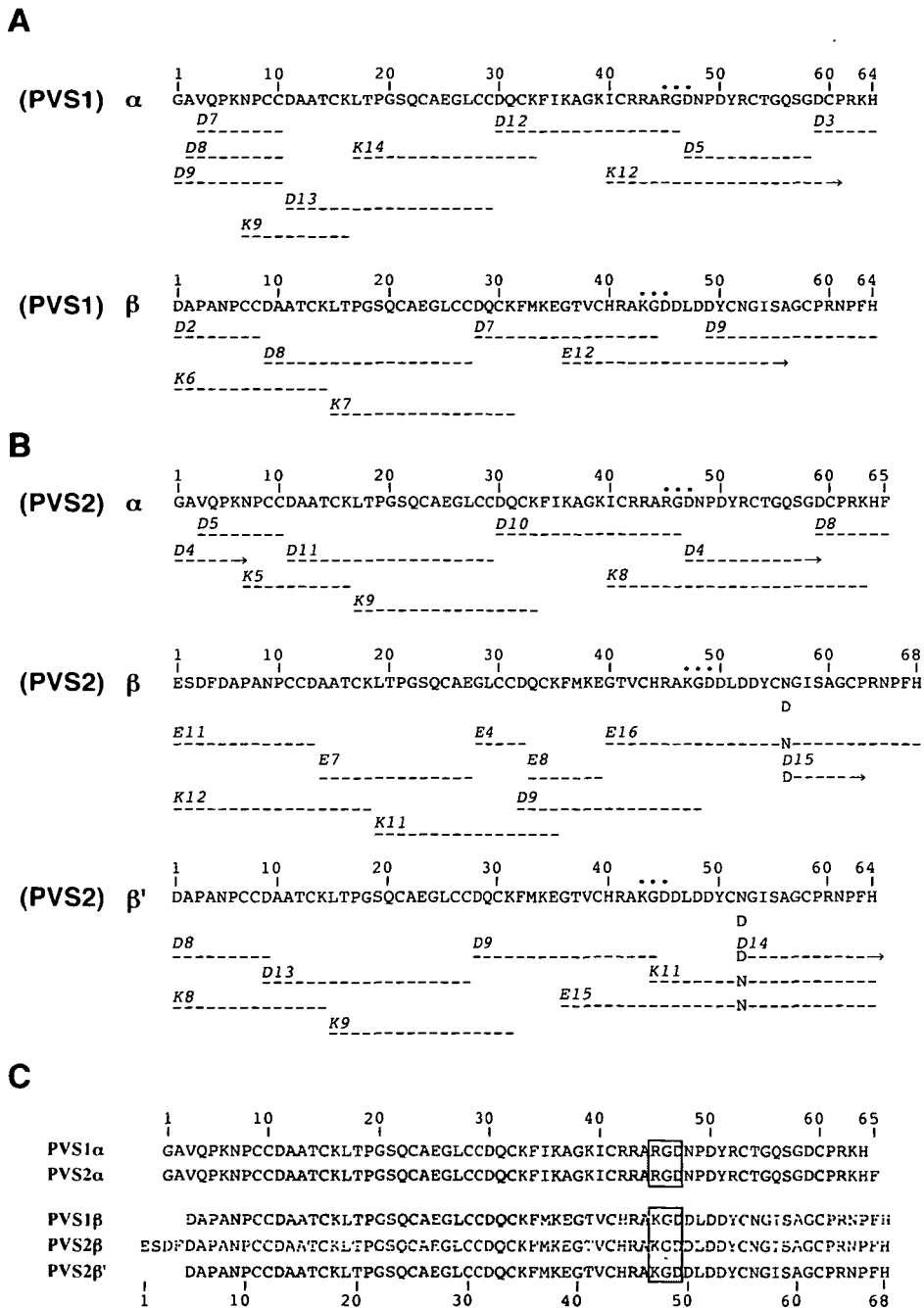


Fig. 2. *S*-Pyridylethylation of piscivostatin 2. A: *S*-Pyridylethylation of piscivostatin 2 (PVS2, major peak in Fig. 1) was performed as described under "MATERIALS AND METHODS."  $\alpha$ ,  $\beta$ , and  $\beta'$  above the peaks indicate the  $\alpha$ ,  $\beta$ , and  $\beta'$  chains of *S*-pyridylethylated PVS2, respectively. B: SDS-PAGE of the pyridylethylated PVS2  $\alpha$  and  $\beta$  chains. The arrows on the left indicate the  $M_r$  of molecular standards.



**Fig. 3. Determination of the amino acid sequence of piscivostatin.** A and B: The amino acid sequence of PVS was determined by enzymatic digestion of S-pyridylethylated subunits. The positions of amino acid residues determined by Edman degradation are shown by broken lines. D, Asp-N fragments; K, Lys-C fragments; E, Glu-C fragments. Dots show the positions of RGD and KGD alignment. PVS2 showed heterogeneity, i.e. asparagine (N) was substituted by aspartic acid (D) at the 56th position of the  $\beta$  chain and the 52nd position of the  $\beta'$  chain (see the amino acid sequences of Asp-N fragment D15 in the  $\beta$  chain of PVS2, and Asp-N fragment D14 in the  $\beta'$  chain of PVS2). C: The complete amino acid sequences of PVS1 and PVS2, and its degradation products. Amino acids identical among the subunits are shaded. The boxes indicate RGD and KGD alignment.

that it was shorter by one amino acid at the C-terminus of the  $\alpha$  chain and four amino acids at the N-terminus of the  $\beta$  chain (Fig. 3C). Therefore, we considered that PVS1 was a degradation product of PVS2, and that PVS2 ( $\alpha$ ,  $\beta$ ) is the mother piscivostatin species. PVS2 was used in all biological assays in this study, PVS being an abbreviation to piscivostatin.

**Mass Spectrometry of PVS**—The mass of PVS2 was determined by matrix-assisted laser desorption/ionization time-of-flight mass spectrometry (MALDI-TOF MS) with a Voyager-DE (Applied Biosystems). The average molecular mass of intact PVS was 14,197.0 Da. Some signals were detected that corresponded to the mass of N-terminal degraded PVS. These degraded fragments were also iso-

lated from the samples obtained by enzymatic digestion of S-pyridylethylated PVS (Fig. 3). This indicated that PVS is a heterodimeric disintegrin molecule composed of  $\alpha$  and  $\beta$  chains.

**Assaying of Binding of Disintegrins to Platelet GPIIb/IIIa**—The binding of PVS and trimestatin to platelet GPIIb/IIIa was examined by ELISA. The apparent  $K_d$  values for PVS and trimestatin were  $5.6 \pm 0.8$  nM ( $n = 3$ ) and  $8.3 \pm 0.4$  nM ( $n = 3$ ), respectively.

**Platelet Aggregation Inhibitory Activity of PVS Determined by Optical Aggregometry**—PVS and trimestatin inhibited ADP-induced platelet aggregation in human PRP in a dose-dependent manner. The  $IC_{50}$  values for 10  $\mu$ M ADP-induced platelet aggregation of PVS and trimestatin were

103 ± 21 nM (n = 4) and 60 ± 29 nM (n = 4), respectively. ADP-induced platelet aggregates disaggregated with time after 1.5–2 min in both the absence and presence of trimes-tatin (Patterns A and B in Fig. 4). The patterns of ADP-induced platelet aggregation with echistatin treatment were also identical to those observed following treatment with trimes-tatin (data not shown). However, ADP-induced platelet aggregates did not disaggregate in the presence of PVS (Patterns C–E in Fig. 4). The ADP-induced platelet aggregation was not affected by treatment with various concentrations of PVS (20 to 180 nM).

**Platelet Aggregation Inhibitory Activity Determined by Laser Light Scattering**—With the laser-light scattering (LS) method, one can detect small platelet aggregates, which can not be detected on optical aggregometry, and can follow this small platelet aggregation even with higher concentra-

tions of disintegrins. We examined the effects of PVS on 10 μM ADP-induced platelet aggregation by monitoring the numbers of small, medium-sized, and large aggregates using a LS method. Figure 5 shows typical results as to the changes in light scattering intensity (LSI) indicating small

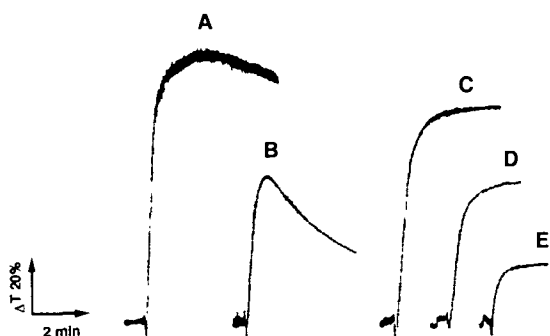


Fig. 4. Platelet aggregation assaying with disintegrins by optical turbidimetry. Platelet aggregation inhibitory activity was assayed by optical turbidimetry. Each disintegrin was added to platelets (PRP) at 37°C. The platelets were activated with ADP (10 μM) after 1 min. (A) 10 μM ADP alone (control). (B) Treatment with trimes-tatin (50 nM). (C) Treatment with PVS (20 nM). (D) Treatment with PVS (100 nM). (E) Treatment with PVS (180 nM).

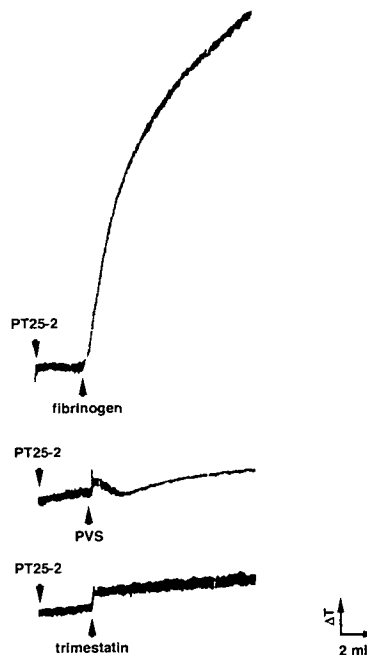


Fig. 6. Effects of piscivostatin on PT25-2-treated washed platelets. Washed platelets were incubated with PT25-2 (10 μg/ml) for 3 min at 37°C with stirring. After incubation, fibrinogen (1 mg/ml), PVS (200 nM), or trimes-tatin (100 nM) was added to the washed platelets, and then the changes in light transmittance were measured. The arrows indicate the points of addition of PT25-2 and disintegrin, respectively.

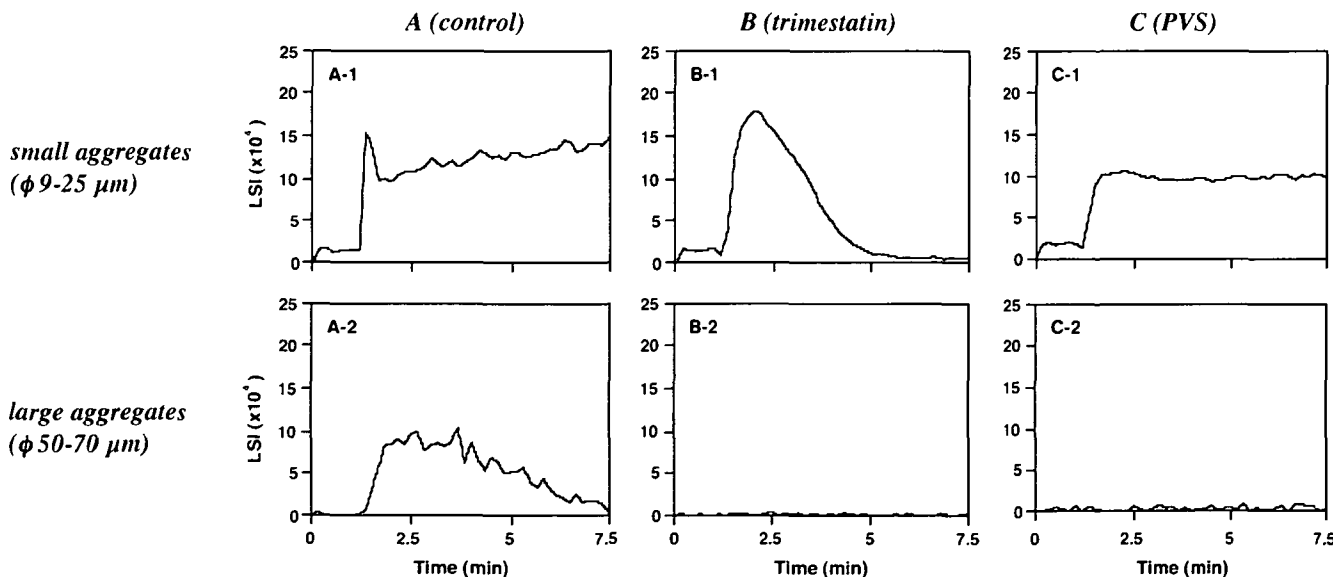


Fig. 5. Platelet aggregation assaying with disintegrins by laser light scattering. Each disintegrin was added to platelets (PRP) at 37°C with stirring at 0 min. One minute after starting the measurement, 10 μM ADP was added to induce platelet aggregation. The light

scattering intensities (LSI) of small and large aggregates were detected in the same samples at the same time. A, no treatment (control); B, treatment with trimes-tatin (100 nM); C, treatment with piscivostatin (200 nM).

and large aggregates after stimulation with ADP. Stimulation with 10  $\mu\text{M}$  ADP alone at 1 min induced rapid formation of small aggregates up to  $15.3 \times 10^4$  LSI arbitrary units (Panel A-1 in Fig. 5). Large aggregates were also rapidly formed, following the small aggregates, and reached  $8 \times 10^4$  LSI arbitrary units (Panel A-2 in Fig. 5). Medium-sized aggregates were also rapidly formed, following the small aggregates, and reached  $12 \times 10^4$  LSI arbitrary units (data not shown). After 1 min 30 s, the level of small aggregates decreased due to the conversion of small aggregates to large ones. Then, the levels of large aggregates decreased slowly after reaching the maximal values, indicating dissociation of these aggregates.

Panels B-1 and B-2 of Fig. 5 show the aggregation patterns of trimegestatin-pretreated platelets stimulated with 10  $\mu\text{M}$  ADP. Small aggregates were rapidly formed on ADP-stimulation until 2 min. Then, these aggregates gradually dissociated, the basal level being reached at 5 min (Panel B-1 in Fig. 5). Trimegestatin completely inhibited the formation of medium-sized (data not shown) and large aggregates (Panel B-2 in Fig. 5).

The patterns of ADP-induced platelet aggregation in the presence of PVS are shown in panels C-1 and C-2 of Fig. 5. LSI indicated that the small aggregates maintained their association (Panel C-1 in Fig. 5). Two hundred nanomolar PVS also completely inhibited the formation of the medium-sized (data not shown) and large aggregates (Panel C-2

in Fig. 5), similar to in the case of trimegestatin-treated platelet aggregation. When lower concentrations of disintegrins were added for ADP-induced platelet aggregation, the formation of small and large aggregates gradually increased, but the patterns of trimegestatin and PVS treated platelet aggregation did not change (data not shown).

**Characterization of the Effect of PVS on PT25-2-Treated Platelets**—To further investigate the characteristic activity of PVS toward ADP-induced platelet aggregation, we used an anti-GPIIb/IIIa monoclonal antibody, PT25-2. This antibody causes a change in the GPIIb/IIIa conformation without platelet activation. PT25-2 induces the binding of ligands such as fibrinogen and disintegrin to GPIIb/IIIa (24). We examined the effects of disintegrins on PT25-2-treated platelets by means of both optical aggregometry and light scattering detection.

PT25-2-treated washed platelets aggregated on the addition of fibrinogen. As shown in Fig. 6, the light transmittance did not change for PT25-2-treated platelets on the addition of trimegestatin. However, PVS caused a slight platelet shape change. These differences in the effects of disintegrins on PT25-2-treated platelets were reproducible in three independent experiments. In the same experiments performed with LS detection, neither disintegrin induced the formation of small aggregates of PT25-2-treated platelets (data not shown).

In the next study, we added excess amounts of the two

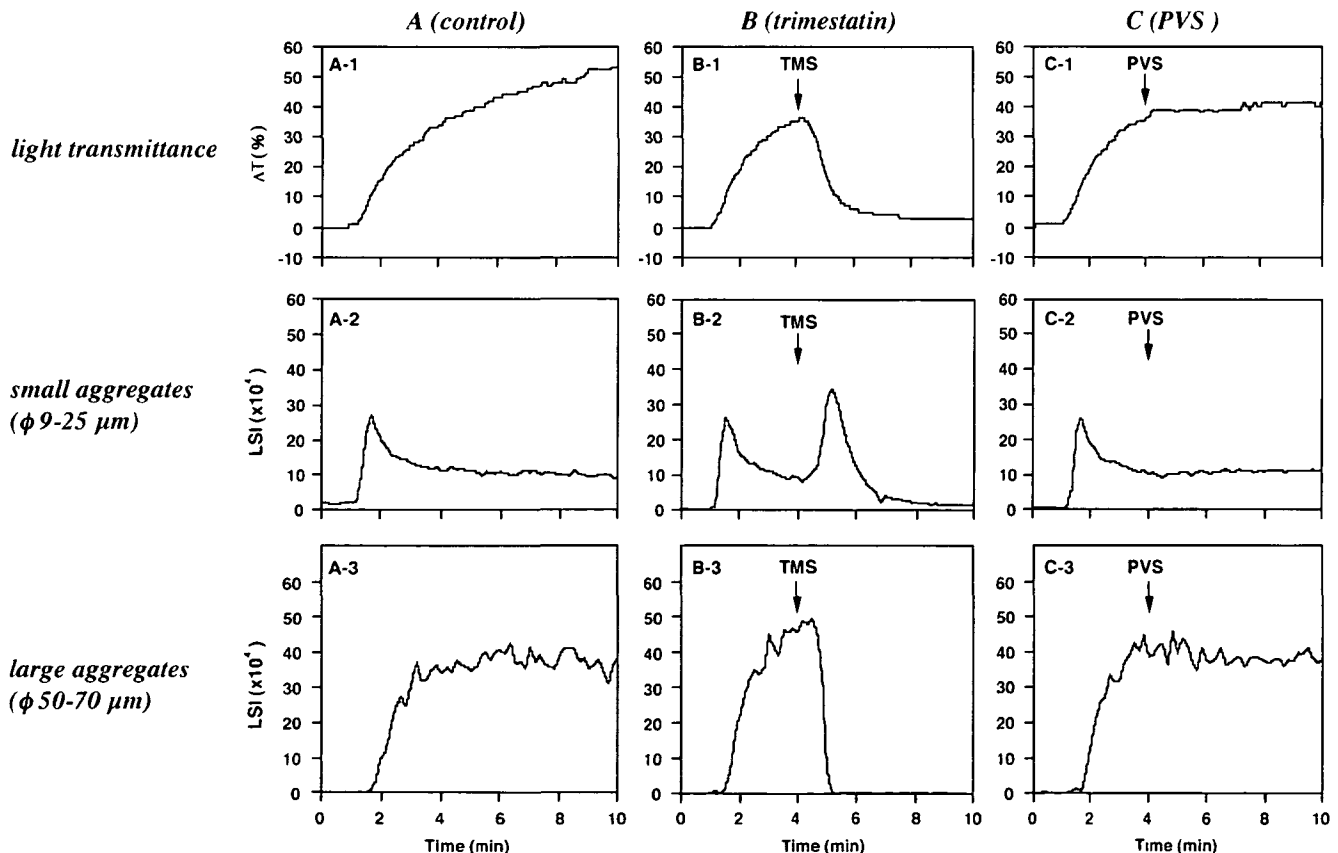


Fig. 7. Effects of excess inhibitors on fibrinogen-induced platelet aggregation. Washed platelets were preincubated with PT25-2 (10  $\mu\text{g}/\text{ml}$ ) for 3 min before measurement at 37°C with stirring. Platelet aggregation was induced by the addition of human fibrinogen (1

mg/ml) at 1 min and then each disintegrin was added to the platelets at 4 min (arrow). The light transmittance and LSI were measured in the same samples at the same time. A, no addition (control); B, trimegestatin (4  $\mu\text{M}$ ); C, PVS (4  $\mu\text{M}$ ).

disintegrins to fibrinogen-induced aggregates of PT25-2 pretreated platelets at 4 min (Fig. 7). The addition of trimestatin induced rapid dissociation of large aggregates into medium-sized and small ones (Panels B-2 and B-3 in Fig. 7). The pattern of medium-sized aggregates was the same as that of large aggregates (data not shown). The LSI level of small aggregates rapidly increased due to the conversion of large and medium-sized aggregates to small ones. Then, the small aggregates completely dissociated by 8 min (Panel B-2 in Fig. 7). The addition of PVS, in contrast, not only stopped fibrinogen-induced platelet aggregation, but also maintained the LSI levels and light transmittance (Panels C-1 to C-3 in Fig. 7).

DISCUSSION

In this study, we isolated and characterized a novel dimeric disintegrin, piscivostatin (PVS), from the venom of *A. piscivorus piscivorus*. The inhibitory effect of PVS on ADP-induced platelet aggregation was quite different from that of the monomeric disintegrin trimestatin.

We have isolated PVS2 and other PVS derivatives. PVS1 lacks one residue at the C-terminal of the PVS2  $\alpha$  chain and four residues at the N-terminal of the PVS2  $\beta$  chain. The  $\beta$  chain of PVS1 is identical to the  $\beta'$  chain of PVS2. Heterogeneity was detected in the amino acid sequence of the  $\beta$  chain of PVS2; an asparagine residues is substituted by aspartic acid at the 56th position of the  $\beta$  chain and the 52nd position of the  $\beta'$  chain (Fig. 3B). However, there were no differences in the inhibitory activities,  $IC_{50}$  or aggregation inhibitory patterns between PVS1 and PVS2. We used PVS2 as piscivostatin in this study.

In Fig. 8, two dimeric disintegrins (piscivostatin and EMF10) and four monomeric disintegrins (flavoridin, applaggin, triflavin, and trimestatin) are presented to compare the amino acid sequences and the locations of disulfide bridges of dimeric disintegrin EMF10 and monomeric disintegrin flavoridin. Marcinkiewicz *et al.* recently isolated other heterodimeric disintegrins, EC3 and EMF10, from *Echis sochureki* (29) and *Eristocophis macmahoni* venom

(23), respectively. EC3 has no RGD sequence and shows no inhibitory effect on platelet aggregation (the amino acid sequence of EC3 is not shown in Fig. 8). EMF10 has one RGD sequence in the A chain and shows a weak platelet aggregation inhibitory effect (29). Applaggin, which was isolated from the venom of *A. piscivorus piscivorus*, had been reported to be a dimeric disintegrin; its apparent molecular mass is 16 kDa under nonreducing conditions and 8 kDa under reducing conditions on SDS-PAGE (30). However, Wencel-Drake *et al.* suggested that applaggin does not have a dimeric structure based on the results of mass spectroscopy (31). Oshikawa and Terada reported a homodimeric disintegrin, ussuristatin 2 (US-2), from the venom of *A. ussuriensis* (22). US-2 had the KGD sequence, and its apparent molecular mass was estimated to be 30 kDa under non-reducing conditions and 8 kDa under reducing conditions on SDS-PAGE. The molecular mass of US-2 was determined to be 16 kDa by analytical gel filtration, suggesting that US-2 is a homodimeric disintegrin (the amino acid sequence of US-2 is not shown) (22).

Trimestatin, which was isolated from the venom of *T. flavoviridis* in our laboratory for use for the control of monomeric disintegrin in all experiments, has an identical amino acid sequence to triflavin, isolated from the same venom, except for the amino acid substitution of 69Gly to 69Asp (26).

Piscivostatin (PVS) has an RGD-/KGD-containing heterodimeric structure and its amino acid sequence is different from those of other known dimeric disintegrins. Each chain of PVS exhibits a high degree of identity to other monomeric disintegrins. The amino termini of PVS start four and two residues, in the  $\alpha$  and  $\beta$  chains, downstream from those of other disintegrins such as flavoridin and triflavin. As shown in Fig. 8B, the alignment of the cysteine residues in PVS was identical of those in other disintegrins except for two cysteine residues in the N-terminal region. The disulfide bond localization of flavoridin was determined by NMR (17), as shown in Fig. 8B. Calvete *et al.* recently determined the localization of the disulfide bonds of EMF10 (lower figure in Fig. 8A); two chains of EMF10 are

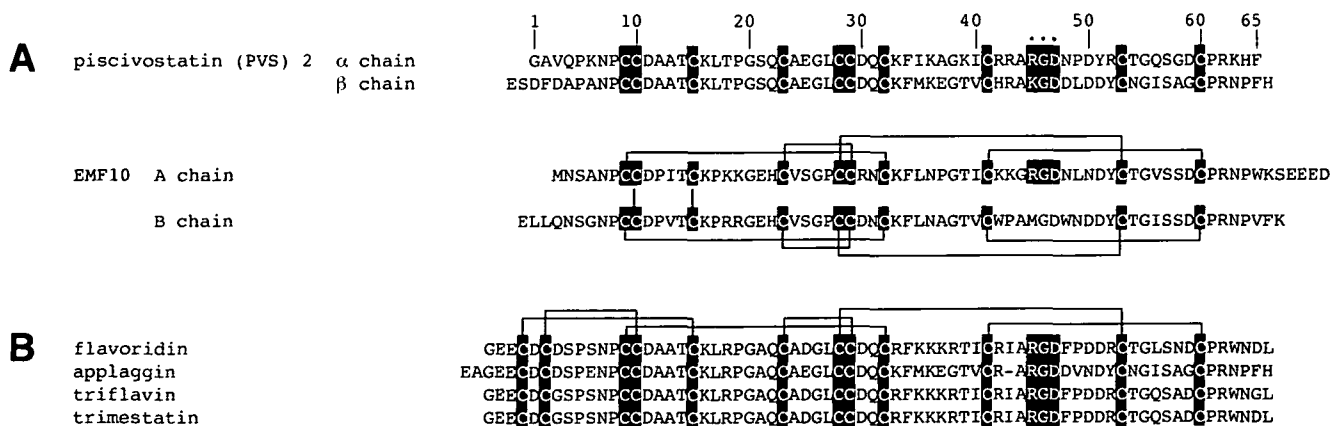


Fig. 8. Comparison of the amino acid sequences of piscivostatin and other disintegrins. A, dimeric disintegrins containing 10 cysteine residues; B, monomeric disintegrins containing 12 cysteine residues. The cysteine residues, and the alignment of RGD and KGD sequences are indicated in reversed letters. The dots above the amino acids indicate the positions of RGD and KGD alignments. The disul-

fide bridges shown by solid lines are derived from those of EMF10 and flavoridin. EMF10 (23, 32) from *E. macmahoni* represents a heterodimeric disintegrin. Flavoridin (17), triflavin (26), and trimestatin, which was isolated and characterized in our laboratory, from *T. flavoviridis*, and applaggin (30) from *A. piscivorus piscivorus* are monomeric disintegrins.

joined by two disulfide bridges through Cys 8 of the A chain and Cys 11 of the B chain, and Cys 13 of the A chain and Cys 16 of the B chain (32). The alignment of cysteine residues in PVS was identical to that in the case of EMF10. Therefore, the locations of disulfide bonds of PVS are most likely identical to those in the case of EMF10.

The apparent  $K_d$  values of PVS and trimestatin binding to platelet GPIIb/IIIa were essentially the same. However, the effect of PVS on platelet aggregation was quite different from that of monomeric disintegrins (Figs. 4 and 5). Both PVS and trimestatin markedly inhibited the formation of small, medium-sized and large aggregates in a dose-dependent manner. The small aggregates of trimestatin-treated platelets then disaggregated with time (Figs. 4B and 5B-1). However, no disaggregation of PVS-treated platelets was observed (Figs. 4C and 5C-1).

These results suggested that PVS might bridge individual platelets through RGD/KGD sequences of PVS and its recognition site on platelet GPIIb/IIIa. The biological activity of PVS toward ADP-induced platelet aggregation is similar to the action of fibrinogen, which binds to GPIIb/IIIa through multiple RGD motifs. Thus, PVS may have fibrinogen-like activity and the PVS-bridged platelet aggregates could not be detached due to the high affinity of PVS for GPIIb/IIIa.

Furthermore, we also isolated another RGD/RGD-containing dimeric disintegrin (designated as acostatin), which has the RGD sequence in each chain (33). The effect of acostatin on ADP-induced platelet aggregation was identical to that of PVS, and also there was no significant difference in the apparent  $K_d$  values for GPIIb/IIIa between PVS and acostatin (unpublished observation). We concluded that the KGD sequence of PVS is not essential for the two contradictory activities; as a platelet aggregation inhibitor and as an effector to induce irreversible platelet aggregation.

To determine whether or not RGD- and KGD-containing PVS has fibrinogen-like effects on ADP-induced platelet aggregation, we examined the effects of a specific anti-GPIIb/IIIa monoclonal antibody, PT25-2, on platelet aggregation. PT25-2 induces a conformational change of GPIIb/IIIa to a ligand-accessible form without platelet activation (24). Trimestatin had no effect on PT25-2-treated washed platelets, whereas PVS induced a shape change alone, as determined on optical aggregometry (Fig. 6). With LS detection, no aggregates were detected on treatment either with PVS or trimestatin (data not shown), suggesting that PVS could not bind to two individual platelets, and also suggesting that PVS does not have a sufficient molecular length to bridge individual platelets unlike fibrinogen. When we added an excess amount of trimestatin at 3 min after fibrinogen-induced platelet aggregation had started, the platelet aggregates dissociated (Fig. 7B). However, a fifteen-fold excess amount of trimestatin had no effect on PVS-treated platelet aggregates on both ADP-induced and PT25-2-pretreated fibrinogen-induced platelet aggregation (data not shown). The addition of an excess amount of PVS stopped both the aggregation and dissociation of platelet aggregates (Fig. 7C), indicating that PVS did not bind to distinct platelets, but that it might have a specific ability to cause the irreversible platelet aggregation.

The mechanism by which PVS does not induce the dissociation of platelet aggregates remains to be determined. The following hypothesis may explain the characteristic

effect of PVS on platelet aggregation. PVS is not able to displace bound fibrinogen like monomeric disintegrin (trimestatin), possibly due to its large molecular size, but the binding of dimeric disintegrin (PVS), which might cause clustering of GPIIb/IIIa on the platelet membrane, induces some outside-in signal transduction resulting in irreversible binding between fibrinogen and GPIIb/IIIa. Hato *et al.* showed that the clustering of GPIIb/IIIa increased irreversible ligand binding to GPIIb/IIIa (34). In addition, Clark *et al.* showed that the platelet signal transduction through tyrosine phosphorylation of a dimeric disintegrin, controstatin, differed from that of a monomeric disintegrin, multisquamatin (35). The shape change of PT25-2-treated platelets was induced by PVS alone. These observations suggested that PVS transmits some characteristic outside-in signal to platelets *via* activated platelet GPIIb/IIIa. This suggestion is in agreement with the previous report of Law *et al.*, indicating that the outside-in signal derived form of cytoplasmic tyrosine motifs of GPIIb/IIIa stabilizes platelet aggregates (36). The characteristic effect of PVS on platelet aggregation might be concerned with GPIIb/IIIa clustering and outside-in signal transduction on platelets.

In summary, we purified and determined the amino acid sequence of a novel RGD/KGD-containing heterodimeric disintegrin, piscivostatin (PVS), from the venom of *A. piscivorus piscivorus*. This is the first demonstration of the characteristic effect of dimeric disintegrins on platelets, which act as inhibitors of platelet aggregation and also as effectors causing irreversible platelet aggregation, as judged with a laser light scattering method, although the precise molecular mechanisms of the events involved in platelet activation remain to be elucidated. In particular, the mechanisms of platelet aggregate dissociation in the reversible phase are scarcely known. However, the present results indicate that piscivostatin (PVS) is a useful tool for studying platelet functions such as the initial events including the signal pathway and post-activating events of platelet aggregation.

We wish to thank Dr. M. Handa for generously donating the PT25-2, Dr. T. Yokoyama for the assistance in the measurement of platelet aggregation by laser light scattering, Drs. M. Moroi and Y. Ozaki for suggesting experiments involving anti-GPIIb/IIIa monoclonal antibodies, and Fumiko Hyodo, Kyoko Kawakita, and Masako Miyawaki for their help with the purification and assays.

## REFERENCES

- George, J.N. and Colman, R.W. (2001) Overview of platelet structure and function in *Hemostasis and Thrombosis: Basic Principles and Clinical Practice*, 4th ed., pp. 381–386 (Colman, R.W., Hirsh, J., Marder, V.J., Clowes, A.W., and George, J.N., eds.) Lippincott Williams and Wilkins, Philadelphia, PA, USA
- Gartner, T.K. and Bennett, J.S. (1985) The tetrapeptide analogue of the cell attachment site of fibronectin inhibits platelet aggregation and fibrinogen binding to activated platelets. *J. Biol. Chem.* **260**, 11891–11894
- Plow, E.F., Pierschbacher, M.D., Ruoslahti, E., Marguerie, G.A., and Ginsberg, M.H. (1985) The effect of Arg-Gly-Asp-containing peptides on fibrinogen and von Willebrand factor binding to platelets. *Proc. Natl. Acad. Sci. USA* **82**, 8057–8061
- D'Souza, S.E., Ginsberg, M.H., and Plow, E.F. (1991) Arginyl-glycyl-aspartic acid (RGD): a cell adhesion motif. *Trends Biochem. Sci.* **16**, 246–250
- Gould, R.J., Polokoff, M.A., Friedman, P.A., Huang, T.F., Holt, J.C., Cook, J.J., and Niewiarowski, S. (1990) Disintegrins: a



- family of integrin inhibitory proteins from viper venoms. *Proc. Soc. Exp. Biol. Med.* **195**, 168–171
6. Huang, T.F. and Niewiarowski, S. (1994) Disintegrins: the naturally-occurring antagonists of platelet fibrinogen receptor. *J. Toxicol.* **13**, 253–273
  7. Niewiarowski, S., McLane, M.A., Kloczewiak, M., and Stewart, G.J. (1994) Disintegrins and other naturally occurring antagonists of platelet fibrinogen receptors. *Semin. Hematol.* **31**, 289–300
  8. Staiano, N., Della Morte, R., Di Domenico, C., Tafuri, S., Squillacioti, C., Belisario, M.A., and Di Natale, P. (1997) Echistatin inhibits pp72syk and pp125FAK phosphorylation in fibrinogen-adherent platelets. *Biochimie* **79**, 769–773
  9. Staiano, N., Garbi, C., Squillacioti, C., Esposito, S., Di Martino, E., Belisario, M.A., Nitsch, L., and Di Natale, P. (1997) Echistatin induces decrease of pp125FAK phosphorylation, disassembly of actin cytoskeleton and focal adhesions, and detachment of fibronectin-adherent melanoma cells. *Eur. J. Cell Biol.* **73**, 298–305
  10. Gan, Z.R., Gould, R.J., Jacobs, J.W., Friedman, P.A., and Polokoff, M.A. (1988) Echistatin. A potent platelet aggregation inhibitor from the venom of the viper, *Echis carinatus*. *J. Biol. Chem.* **263**, 19827–19832
  11. Scarborough, R.M., Rose, J.W., Hsu, M.A., Phillips, D.R., Fried, V.A., Campbell, A.M., Nannizzi, L., and Charo, I.F. (1991) Barbourin. A GPIIb-IIIa-specific integrin antagonist from the venom of *Sistrurus m. barbouri*. *J. Biol. Chem.* **266**, 9359–9362
  12. Huang, T.F., Holt, J.C., Lukasiewicz, H., and Niewiarowski, S. (1987) Trigramin. A low molecular weight peptide inhibiting fibrinogen interaction with platelet receptors expressed on glycoprotein IIb-IIIa complex. *J. Biol. Chem.* **262**, 16157–16163
  13. Dennis, M.S., Henzel, W.J., Pitti, R.M., Lipari, M.T., Napier, M.A., Deisher, T.A., Bunting, S., and Lazarus, R.A. (1990) Platelet glycoprotein IIb-IIIa protein antagonists from snake venoms: evidence for a family of platelet-aggregation inhibitors. *Proc. Natl. Acad. Sci. USA* **87**, 2471–2475
  14. Shebuski, R.J., Ramjit, D.R., Bencen, G.H., and Polokoff, M.A. (1989) Characterization and platelet inhibitory activity of bitistatin, a potent arginine-glycine-aspartic acid-containing peptide from the venom of the viper *Bitis arietans*. *J. Biol. Chem.* **264**, 21550–21556
  15. Calvete, J.J., Wang, Y., Mann, K., Schafer, W., Niewiarowski, S., and Stewart, G.J. (1992) The disulfide bridge pattern of snake venom disintegrins, flavoridin and echistatin. *FEBS Lett.* **309**, 316–320
  16. Saudek, V., Atkinson, R.A., Lepage, P., and Pelton, J.T. (1991) The secondary structure of echistatin from <sup>1</sup>H-NMR, circular dichroism and Raman spectroscopy. *Eur. J. Biochem.* **202**, 329–338
  17. Senn, H. and Klaus, W. (1993) The nuclear magnetic resonance solution structure of flavoridin, an antagonist of the platelet GP IIb-IIIa receptor. *J. Mol. Biol.* **232**, 907–925
  18. Adler, M., Carter, P., Lazarus, R.A., and Wagner, G. (1993) Cysteine pairing in the glycoprotein IIb/IIIa antagonist kistrin using NMR, chemical analysis, and structure calculations. *Biochemistry* **32**, 282–289
  19. Calvete, J.J., Schrader, M., Raida, M., McLane, M.A., Romero, A., and Niewiarowski, S. (1997) The disulphide bond pattern of bitistatin, a disintegrin isolated from the venom of the viper *Bitis arietans*. *FEBS Lett.* **416**, 197–202
  20. Trikha, M., Rote, W.E., Manley, P.J., Lucchesi, B.R., and Markland, F.S. (1994) Purification and characterization of platelet aggregation inhibitors from snake venoms. *Thromb. Res.* **73**, 39–52
  21. Zhou, Q., Hu, P., Ritter, M.R., Swenson, S.D., Argounova, S., Epstein, A.L., and Markland, F.S. (2000) Molecular cloning and functional expression of contortrostatin, a homodimeric disintegrin from southern copperhead snake venom. *Arch. Biochem. Biophys.* **375**, 278–288
  22. Oshikawa, K. and Terada, S. (1999) Ussuristatin 2, a novel KGD-bearing disintegrin from *Agkistrodon ussuriensis* venom. *J. Biochem.* **125**, 31–35
  23. Marcinkiewicz, C., Calvete, J.J., Vijay-Kumar, S., Marcinkiewicz, M.M., Raida, M., Schick, P., Lobb, R.R., and Niewiarowski, S. (1999) Structural and functional characterization of EMF10, a heterodimeric disintegrin from *Eristocophis macmahoni* venom that selectively inhibits  $\alpha 5 \beta 1$  integrin. *Biochemistry* **38**, 13302–13309
  24. Tokuhira, M., Handa, M., Kamata, T., Oda, A., Katayama, M., Tomiyama, Y., Murata, M., Kawai, Y., Watanabe, K., and Ikeda, Y. (1996) A novel regulatory epitope defined by a murine monoclonal antibody to the platelet GPIIb-IIIa complex ( $\alpha$  IIb  $\beta$  3 integrin). *Thromb. Haemost.* **76**, 1038–1046
  25. Phillips, D.R., Fitzgerald, L.A., Parise, L.V., and Steiner, B. (1991) Platelet membrane glycoprotein IIb-IIIa complex: Purification, characterization, and reconstitution into phospholipid vesicles. *Methods Enzymol.* **215**, 246–251
  26. Huang, T.F., Sheu, J.R., Teng, C.M., Chen, S.W., and Liu, C.S. (1992) Triflavin, an antiplatelet Arg-Gly-Asp-containing peptide, is a specific antagonist of platelet membrane glycoprotein IIb-IIIa complex. *J. Biochem.* **109**, 328–334
  27. Schagger, H. and von Jagow, G. (1987) Tricine-sodium dodecyl sulfate-polyacrylamide gel electrophoresis for the separation of proteins in the range from 1 to 100 kDa. *Anal. Biochem.* **166**, 368–379
  28. Ozaki, Y., Satoh, K., Yatomi, Y., Yamamoto, T., Shirasawa, Y., and Kume, S. (1994) Detection of platelet aggregates with a particle counting method using light scattering. *Anal. Biochem.* **218**, 284–294
  29. Marcinkiewicz, C., Calvete, J.J., Marcinkiewicz, M.M., Raida, M., Vijay-Kumar, S., Huang, Z., Lobb, R.R., and Niewiarowski, S. (1999) EC3, a novel heterodimeric disintegrin from *Echis carinatus* venom, inhibits  $\alpha 4$  and  $\alpha 5$  integrins in an RGD-independent manner. *J. Biol. Chem.* **274**, 12468–12473
  30. Chao, B.H., Jakubowski, J.A., Savage, B., Chow, E.P., Marzec, U.M., Harker, L.A., and Maraganore, J.M. (1989) *Agkistrodon piscivorus piscivorus* platelet aggregation inhibitor: a potent inhibitor of platelet activation. *Proc. Natl. Acad. Sci. USA* **86**, 8050–8054
  31. Wencel-Drake, J.D., Frelinger, A.L. 3rd, Dieter, M.G., and Lam, S.C. (1993) Arg-Gly-Asp-dependent occupancy of GPIIb/IIIa by applaggin: evidence for internalization and cycling of a platelet integrin. *Blood* **81**, 62–69
  32. Calvete, J.J., Jurgens, M., Marcinkiewicz, C., Romero, A., Schrader, M., and Niewiarowski, S. (2000) Disulphide-bond pattern and molecular modelling of the dimeric disintegrin EMF-10, a potent and selective integrin  $\alpha 5 \beta 1$  antagonist from *Eristocophis macmahoni* venom. *Biochem. J.* **345**, 573–581
  33. Okuda, D. and Morita, T. (1999) Determination of amino acid sequence of dimeric disintegrin (in Japanese). *Seihagaku* **71**, 732
  34. Hato, T., Pampori, N., and Shattil, S.J. (1998) Complementary roles for receptor clustering and conformational change in the adhesive and signaling functions of integrin  $\alpha$ IIb  $\beta$ 3. *J. Cell Biol.* **141**, 1685–1695
  35. Clark, E.A., Trikha, M., Markland, F.S., and Brugge, J.S. (1994) Structurally distinct disintegrins contortrostatin and multi-squamatin differentially regulate platelet tyrosine phosphorylation. *J. Biol. Chem.* **269**, 21940–21943
  36. Law, D.A., DeGuzman, F.R., Heiser, P., Ministri-Madrid, K., Killeen, N., and Phillips, D.R. (1999) Integrin cytoplasmic tyrosine motif is required for outside-in  $\alpha$ IIb $\beta$ 3 signalling and platelet function. *Nature* **401**, 808–811